Raman and infrared investigations of glass and glass-ceramics with composition $2Na_2O \cdot 1CaO \cdot 3SiO_2$

Ervino C. Ziemath
Departamento de Física, IGCE, Universidade Estadual Paulista, Cx. Postal 178, 13500-230-Rio Claro, SP, Brazil

Michel A. Aegerter
Instituto de Física e Química de São Carlos, Universidade de São Paulo, Cx. Postal 369, 13560-970-São Carlos, SP, Brazil

(Received 5 November 1992; accepted 27 August 1993)

Precursor glass and glass-ceramics with molar composition $2Na_2O \cdot 1CaO \cdot 3SiO_2$ are studied by infrared, conventional, and microprobe Raman techniques. The Gaussian deconvoluted Raman spectrum of the glass presents bands at 625 and 660 cm^{-1}, attributed to bending vibrations of Si–O–Si bonds, and at 860, 920, 975, and 1030 cm^{-1}, attributed to symmetric stretching vibrations of SiO_4 tetrahedra with 4, 3, 2, and 1 nonbridging oxygens, respectively. The Raman microprobe spectrum of a highly crystallized sample presents two narrow and intense bands at about 590 and 980 cm^{-1}, associated with vibrations of SiO_4 tetrahedra with two nonbridging oxygens, in agreement with the predicted chain-like structure of crystalline metasilicates. Scanning electron microscopy shows that the crystals distributed in partially crystallized samples have a spherical shape, built up by radially oriented needle-like single crystals. The Raman microprobe spectra of these spherulites show that they still contain residual amorphous material. A comparison of Raman and infrared spectra of amorphous and highly crystallized samples is presented.

I. INTRODUCTION

Raman and infrared spectroscopic techniques are widely used to investigate vibrational modes of crystalline and amorphous solids. However, there is no way to determine the structural arrangement of solids directly from the measured vibrational spectra.

The structure of glasses is characterized by a lack of long-range order due to a distribution of the bond lengths and bond angles.[1] Consequently, there is a breakdown of Raman scattering selection-rules[2] known for single crystals and isolated simple molecules.[3] The correlation of the different types of interatomic bond vibrations with the respective frequency of the infrared and Raman bands needs some knowledge about the nature of these bonds and the structural arrangement of the atoms in the material.

The present paper deals with Raman spectroscopy of glass and glass ceramics with molar composition $2Na_2O \cdot 1CaO \cdot 3SiO_2$, called hereafter N_2CS_3. With additional measurements of infrared spectroscopy and x-ray diffraction, and scanning electron microscopy observations, we were able to correlate the microstructure of these materials with some of their vibrational modes.

Section II presents some relevant data about the nucleation and crystal growth in N_2CS_3 glass and comments on scanning electron microscopy observations. The experimental procedures, like sample preparation, employed equipment, and experimental techniques are presented in Sec. III. Section IV is dedicated to the exposure and discussion of the results obtained with x-ray diffraction, infrared, conventional, and microprobe Raman spectroscopy measurements; it also presents a discussion about surface composition of the glass through a comparison of Raman spectra of other simple metasilicate glasses. Section V is devoted to the conclusions of this work.

II. THE $2Na_2O \cdot 1CaO \cdot 3SiO_2$ GLASS AND GLASS-CERAMICS

The N_2CS_3 glass investigated belongs to the metasilicate class and can be transformed in glass-ceramics by controlled thermal treatment. Quantitative studies of the nucleation and crystal growth have been performed by Fokin *et al.*[4–6] The glass undergoes homogeneous nucleation between 440 and 570 °C, with a maximum nucleation rate at 505 °C.

Table I lists the activation enthalpies, ΔH, for steady-state nucleation, crystal growth, viscous flow, and glass transition, and the temperature range of these thermal processes which occur in the glass.

Scanning electron microscopy observations of partially crystallized samples show that the crystals grown in the glass matrix are spherical [Fig. 1(a)]. They are built up by needle-like crystals mainly radially oriented.

Aeg 224

TABLE I. Temperature ranges and activation enthalpies, ΔH, of various thermal processes occurring in N_2CS_3 glass.

Process	Temperature range (°C)	ΔH (kcal/mol)
Steady-state nucleation[a]	450–498	146
Crystal growth[a]	527–586	102
Viscous flow[a]	462–509	197
Glass transition[b]	462–485	78

[a]Refs. 4–6.
[b]Ref. 7 [from measurements of differential scanning calorimetry (DSC) with heating rates ranging from 5 to 30 °C/min].

These spherical crystals are called spherulites.[8,9] After prolonged thermal treatments, the samples become highly crystallized, as shown in Fig. 1(b).

The microprobe Raman spectra were measured on the same samples shown in Fig. 1. Conventional Raman and infrared measurements were made on amorphous samples. Highly crystallized samples, like that shown in Fig. 1(b), were submitted to x-ray diffraction and infrared measurements.

III. EXPERIMENTAL PROCEDURE

A. Sample preparation

Reagent grade solidum carbonate (Riedel-deHaën), calcium carbonate (Merck), and washed quartz sand AB 90BTF (Mineração Jundu, Brazil) were weighed in adequate proportions to give the N_2CS_3 glass composition. The starting reagents were homogenized in a closed glass vessel via manual shaking. The material was then transferred to a platinum crucible which was placed in an electrical heated Globar furnace. The temperature was raised from 800 to 1350 °C, and maintained at this temperature for 2 h. Mechanical homogenization was performed with a platinum stirrer (50 rpm). The stirrer was removed from the liquid 1/2 h before casting to allow the diffusion of possible bubbles to the batch surface. As soon as the crucible was withdrawn from the furnace, 40–50 g of the batch was cast on an 8 mm thick iron plate and immediately pressed manually with a 10 mm thick, 100 mm diameter stainless steel disk. This disk was maintained on the hardened ~4 mm thick glass plate until the temperature reaches about 300 °C. Using this protocol the cooling rate was higher than 400 °C/min and fast enough to prevent crystal nucleation which takes place between 570 °C and 440 °C,[4–6] as verified by visual and x-ray diffraction inspection. Detailed studies[7] indicate that cooling rates higher than 225 °C/min are in fact fast enough to prevent crystallization in the N_2CS_3 metasilicate glass. The resulting glass was transparent, bubble free, and slightly greenish. This slight coloration was probably due to very small amounts of iron or chromium oxide impurities, but no specific optical absorption band was found between 350 and 1500 nm. Table II gives the theoretical and chemically analyzed compositions.

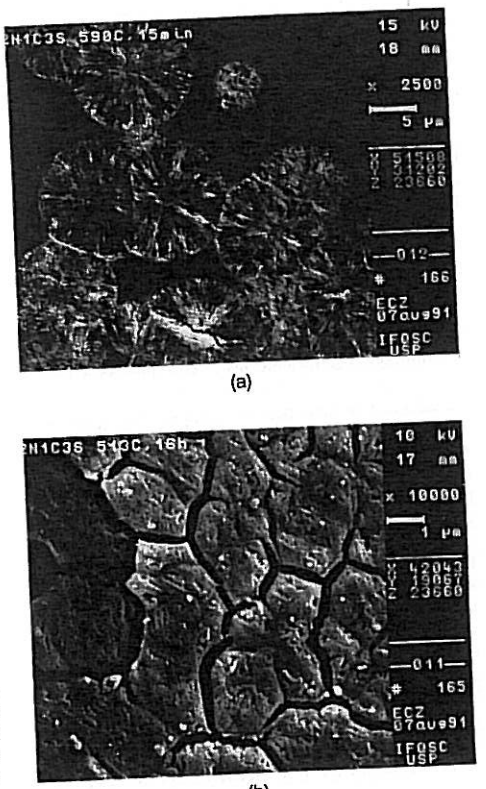

FIG. 1. SEM micrographs of N_2CS_3 samples thermally treated in air at (a) 590 °C for 15 min and (b) 513 °C for 16 h. The observed surfaces of both samples were previously polished, etched in acid solution, and coated with a 10 nm sputtered Au film.

Thermal treatments for crystallization were performed in a horizontal tubular electrical furnace, with temperature stability better than ±1 °C.

TABLE II. Theoretical and chemical determination of the composition of N_2CS_3 glass.

Oxide	Theoretical (wt. %)	Chemical (wt. %)	Method
Na_2O	34.43	34.83 ± 0.001	Flame photometry
CaO	15.35	15.54 ± 0.05	EDTA titulometry
SiO_2	50.22	48.01 ± 0.05	Gravimetry

Samples were ground with several grade SiC powders on plane iron matrices, and then polished to an optical degree with 1.0 μm size Ce_2O_3 on a pitch tool.

B. Equipment

X-ray diffraction data have been obtained for monolithic and powder samples with a Philips and a Rigaku Rotaflex diffractometer using the Cu K_α radiation and a Ni filter (λ = 1.5418 Å).

The microstructure of the glass-ceramic samples was observed with a Zeiss DSM 960 scanning electron microscope. The polished samples were previously etched for 10 s in an aqueous solution of 0.05 vol. % HCl and 0.02 vol. % HF. The surface to be observed was metallized with a 10 nm thick sputtered Au or Pd film.

Infrared spectroscopy was performed on a Nicolet FTIR 5SXC spectrometer. Reflectance spectra were obtained for monolithic polished samples having thickness and diameter of about 1.2 mm and 12 mm, respectively, using a Spectra Tech Inc. Diffuse Reflectance Unit, mod. 0030-001. Transmittance spectra were measured on powder samples pressed in KBr pellets under a uniaxial pressure of about 20 000 psi.

Unpolarized Raman spectra were obtained through two different experimental arrangements: (1) conventional 90° scattering and (2) the microprobe backscattering technique. In the 90° scattering arrangement the samples were excited with the 4880 and 5145 Å lines of a Spectra Physics 171 argon ion laser, and power of about 400 mW. The scattered light was analyzed with a Spex 1402 double spectrometer, in which diffraction gratings of 1200 grooves/mm and blaze at 5000 Å were mounted. The widths of the entrance and exit slits of the spectrometer were fixed at 200 μm, giving a spectral resolution of about 1 cm^{-1}. The analyzed light was detected by a Products for Research C31034-RF water-cooled photomultiplier. The electrical signal was processed digitally.

The Raman spectra of microregions in the sample surfaces have been measured with a DILOR Confocal Laser Raman, Ref. 1.XY.00.C, using the 5145 Å line of an argon ion laser, operating with a power of 100 mW. The microregions to be analyzed were defined with the help of an optical microscope coupled to the spectrometer.

IV. RESULTS AND DISCUSSION

A. X-ray diffraction

Our studies have shown that the N_2CS_3 amorphous samples can be transformed continuously into a polycrystalline material by increasing the thermal treatment time at a fixed temperature.[7] Powder and monolithic polycrystalline samples present the same x-ray diffraction pattern for heat treatment up to 586 °C. This temperature is slightly above the upper limit of nucleation rate curve,[4–6] and below it no crystalline phase transformation was observed.

Figure 2 shows a typical x-ray diffraction pattern, obtained for a monolithic sample heat-treated at 480 °C for 24 h and subsequently at 520 °C for 3 h.

This x-ray diffraction pattern has no similarities with that of other sodium and calcium metasilicates, such as $Na_2O \cdot SiO_2$,[10] $CaO \cdot SiO_2$,[11,12] and $1Na_2O \cdot 2CaO \cdot 3SiO_2$,[13,14] for which the crystalline structure has been determined.

Wyckoff and Morey[15] concluded that the N_2CS_3 crystal does not have a cubic symmetry. Kröger and Blömer[16] reach the same conclusion and affirm that its diffractograms "have a great number of peaks which incapacitate its fitting in the hexagonal, tetragonal, or rhombic systems, as long as higher lattice parameters are not taken into account".

B. Infrared spectra

Infrared spectra of amorphous and polycrystalline N_2CS_3 samples are shown in Fig. 3. The polycrystalline samples [spectra (b) and (d)] have different thermal treatments, but their x-ray diffraction patterns were identical, showing no indication of remainder amorphous phase.

The peaks at 703 and 881 cm^{-1} of spectrum (a) are due to anhydrous Na_2CO_3, which presents bands at 697, 726, and 878 cm^{-1}, and $CaCO_3$, in which bands occur at 710 and 878 cm^{-1}.[17] The presence of these carbonates in the samples is due to surface adsorption of atmospheric CO_2 molecules on the large surface area of the finely ground samples. Atmospheric CO_2 presents an active infrared band at 664 cm^{-1},[17] which appears in the spectrum (c) of Fig. 3.

Water adsorption also occurs, and reacts easily with sodium and calcium ions forming hydroxides. However,

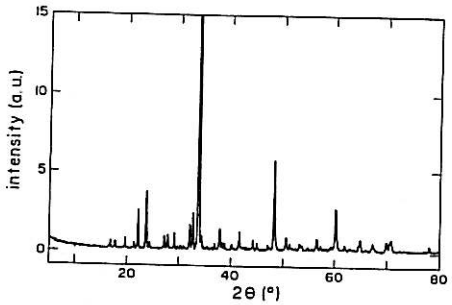

FIG. 2. X-ray diffraction pattern of a monolithic N_2CS_3 sample thermally treated at 480 °C for 24 h plus 520 °C for 3 h.

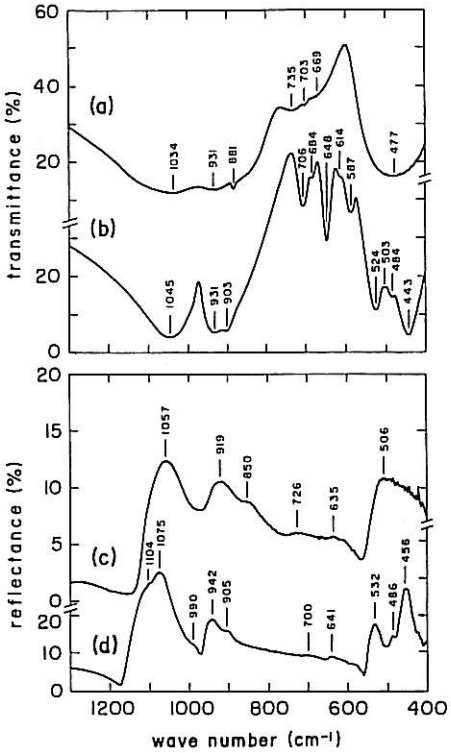

FIG. 3. FTIR spectra of amorphous, (a) and (c), and polycrystalline, (b) and (d), N_2CS_3 samples measured in transmission, (a) and (b), and reflection, (c) and (d). The polycrystalline samples have different thermal treatments: (b) 513 °C, 16 h, and (d) 480 °C, 24 h plus 520 °C, 3 h.

the infrared absorption bands due to OH^- and H_2O occur in the 3400–3700 cm^{-1} range.[18]

Based on literature dealing with infrared spectra of glasses with composition close to sodium disilicate,[19–22] the bands observed for the N_2CS_3 amorphous sample are tentatively attributed to bending of bridging oxygens (BO) at 480 cm^{-1}, symmetric stretching of BO at 630–740 cm^{-1}, symmetric stretching of nonbridging oxygens (NBO) at 800–1050 cm^{-1}, and asymmetric stretching of BO at 1100 cm^{-1}.

The bands observed for N_2CS_3 polycrystalline samples at these frequencies are narrower, and their fine structure is resolved mainly in the 400–730 cm^{-1} range of the transmission spectra (b) and between 420 and 540 cm^{-1} in the reflection spectra (d).

The infrared activity observed between 580 and 750 cm^{-1} is more evident in the transmittance spectra than in the reflectance spectra. These differences are more pronounced for the polycrystalline samples spectra. This behavior can be attributed to the differences between bulk and surface vibration modes. The transmittance spectra give information about the bulk bond vibrations, as the spectra for thin glass films and for finely ground glass powder are essentially the same. This can be seen in the spectra of the $Na_2O \cdot 2SiO_2$ glass film presented by Park and Chen (Fig. 1 in Ref. 19) and $Na_2O \cdot 2.022SiO_2$ glass powder supported by the KBr pellet presented by Sweet and White (curve 3 of Fig. 3 in Ref. 23). On the other hand, the reflectance spectra give essentially the frequencies of surface and near-surface vibrational modes. The optical penetration depth for silicate glasses, though varying significantly with composition and wavelength, is of the order of at least 1 μm.[24] In this way it can be asserted that the structural units responsible for the transmittance bands in this frequency range (580–750 cm^{-1}) are either absent at the surface, or their number is very low. Additionally, the Si–O bond lengths at the surface are shorter than in the bulk, with the surface layer in compression due to absence of attractive electronic forces above the surface,[25] despite the adsorbed moisture. This results in more distorted surface tetrahedra with respect to the bulk ones, and in changes in the force constants of the chemical bonds. As a consequence, frequency shifts occur in a manner which is characteristic to each surface mode,[26] which are clearly observed for amorphous and polycrystalline spectra in Fig. 3.

C. Conventional Raman spectrum and its deconvolution

Figure 4 shows the Raman spectrum of an amorphous N_2CS_3 sample obtained with the conventional 90° scattering geometry.

The low frequency bands at 70 cm^{-1} in the Stokes side and at 66 cm^{-1} in the anti-Stokes side of the spectrum are the "boson peaks" due to thermal phonons.[27,28] As the temperature is lowered, the population of thermal phonons in the sample is reduced, and the intensity of the anti-Stokes boson peak is reduced practically to zero at very low temperatures.[29]

In silicate glasses the bands between 550 and 1200 cm^{-1} are generally attributed to vibrations of bonds in SiO_4 tetrahedra and Si–O–Si bonds linking the tetrahedra.[30] More precisely, the high-frequency bands (800–1200 cm^{-1}) have been attributed to symmetric stretching vibrations of SiO_4 tetrahedra with different numbers of NBO,[31] and the asymmetric band in the midfrequency range (500–700 cm^{-1}) have been attributed to bending vibrations of Si–NBO bonds.[32]

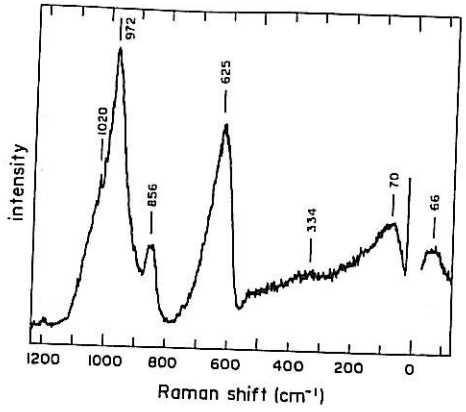

FIG. 4. Unpolarized Raman spectrum of the N_2CS_3 glass sample measured with conventional 90° scattering geometry (λ = 4880 Å, scanning speed: 2.3 cm^{-1}/s).

The weak band around 350 cm^{-1} is usually related to vibrations of the bonds linking the glass modifier cations and the NBO.[33]

Raman spectra of silicate glasses can be deconvoluted in Gaussian curves, as shown by Mysen and co-workers.[32,34] Based on these works the spectrum shown in Fig. 4 was deconvoluted using the Gaussian distribution function:

$$I(\nu) = \frac{A}{\sigma\sqrt{2\pi}} \exp\left[-\frac{1}{2}\left(\frac{\nu - \nu_0}{\sigma}\right)^2\right], \quad (1)$$

where $\nu = \omega/2\pi c$ is the Raman shift in cm^{-1}, ω is the angular frequency of the scattered radiation, c is the light velocity, ν_0 is the Raman shift at which $I(\nu)$ is maximum, σ is the halfwidth at the inflection points, and A is the area under the curve and also a magnification parameter defined by:

$$A = \sigma\sqrt{2\pi} I(\nu_0) \quad (2)$$

The parameters of the six Gaussians obtained by deconvolution are listed in Table III. The individual Gaussians and the sum of them are drawn in Fig. 5(a) and compared with the experimental spectrum in Fig. 5(b).

Each Gaussian should represent a structural unit performing a specific vibrational motion with frequencies inside an interval represented by the base length of the corresponding Gaussian.

At this point, however, no relation can be made between the frequencies of the deconvoluted bands, the type of vibration, and the glass structure. The knowledge of the glass structure gives information about the structural units and, consequently, about the vibrational

TABLE III. Parameters of the individual Gaussians, I_i, indicated in Fig. 5(a), obtained by deconvolution of the experimental Raman spectrum of N_2CS_3 glass.

I_i	ν_{oi} (cm^{-1})	σ_i (cm^{-1})	A_i (a.u.)
I_1	625	26	278.8
I_2	660	50	348.9
I_3	860	20	129.0
I_4	920	22	119.5
I_5	975	23	409.8
I_6	1030	45	442.9

motions which anyone can perform. An important aspect to be considered is that only those vibrations that are accompanied by change in the polarizability of the structural units during the motion contribute substantially to the Raman intensity.[3]

Silica glass is formed by SiO_4 tetrahedra joined together by the oxygens at the corners. Since the Si–O bond lengths and the Si–O–Si and O–Si–O bond

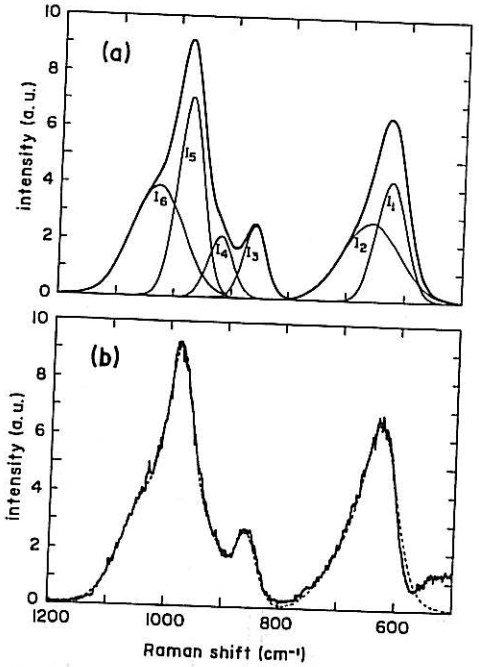

FIG. 5. Deconvolution of the experimental Raman spectrum of N_2CS_3 glass (see Fig. 4) in six Gaussian curves. (a) Individual Gaussians, I_i, and their sum; (b) superposition of the sum of the Gaussians and the measured spectrum.

angles are not constant, but have a distribution about mean values, silica glass has a random three-dimensional network. The addition of modifier cations into this structure breaks some of the Si–O–Si bonds, and NBO, $Si–O^-$ bonds are formed. The modifier cations are coordinated by these oxygens for charge compensation, turning the glass electrically neutral.[35]

In a metasilicate glass, 50 mol % of its composition is constituted by modifier oxides, and all SiO_4 tetrahedra have, on average, two NBO. The structure of those glasses is therefore mainly constituted of SiO_4 chains, joined by the modifier cations. But due to its random nature, SiO_4 tetrahedra with 1, 3, and 4 NBO are also present. Consequently, the main Raman bands of metasilicate glasses have been attributed to vibrations of structural units built up by SiO_4 tetrahedra with different numbers of NBO: SiO_4^{4-} monomers (4NBO), $Si_2O_7^{6-}$ dimers (3NBO), $Si_2O_6^{4-}$ chains and rings (2NBO), and $Si_2O_5^{2-}$ sheets (1NBO).[31] During melting those units are in equilibrium. When the melt is quenched, the reactions stop due to the increase in viscosity. A decrease in the polymerization of the network occurs in glasses containing an increasing amount of modifier oxides, and SiO_2 three-dimensional structural units have a lower probability to be formed during the melt quenching.

In a metasilicate melt the equilibrium of the anionic units can be represented by a reaction of the type:

$$2Si_2O_6^{4-} \leftrightarrows Si_2O_7^{6-} + Si_2O_5^{2-} \quad (3)$$

SiO_4^{4-} monomers are involved in the reaction of dimers and chains which can be written as:

$$2Si_2O_7^{6-} \leftrightarrows 2SiO_4^{4-} + Si_2O_6^{4-} \quad (4)$$

If, during the quenching, the glass retains these anionic units, the four high frequency Gaussian bands of the deconvoluted Raman spectrum of Fig. 5 can be related to vibrations of the four anionic units involved in reactions (3) and (4). The correspondence is shown in Table IV.

The data in Table IV agree well with the proposals of Mysen *et al.*,[31,32] who studied the Raman spectra of the wollastonite glass, $CaO \cdot SiO_2$, a simpler metasilicate. In Sec. IV.E it will be shown that the Raman spectra

TABLE IV. Correspondence of the anionic structures and the frequencies of the Gaussian bands, I_i, in the Raman spectrum of the N_2CS_3 glass.

Anionic structures	Symmetric stretching vibration (cm^{-1})	I_i
SiO_4^{4-}, monomers	860	I_3
$Si_2O_7^{6-}$, dimers	920	I_4
$Si_2O_6^{4-}$, chains or rings	975	I_5
$Si_2O_5^{2-}$, sheets	1030	I_6

of this glass, like other metasilicate glasses, have some similarities with that of N_2CS_3 glass.

The frequency range between 800 and 1200 cm^{-1} is where the infrared spectra [Figs. 3(a) and 3(c)] and Raman spectra (Fig. 4) have higher activity. Indeed, important information can be obtained through a conscientious comparison between these spectra. The most intense Raman band at 972 cm^{-1} has no distinct corresponding infrared band; therefore, the stretching vibration of SiO_4 tetrahedra in the chain structural units (2NBO), associated with the I_5 Gaussian (Fig. 5), is symmetric, as assumed early. On the other hand, the infrared bands located at about 850, 920, and 1030–1060 cm^{-1} have a correspondence with the bands of the deconvoluted Raman spectra located at 860 (I_3), 920 (I_4), and 1030 cm^{-1} (I_6), respectively. This means that the assumed symmetric stretching vibrations of sheets, dimers, and monomer units are slightly perturbed by some asymmetric vibration, probably due to coupling between stretching and bending vibrations of the bridging oxygens. Asymmetric vibrations of tetrahedra molecules present generally a change in the dipole moment of the molecules and are therefore infrared active.

The detailed nature of the vibrations responsible for the 625 cm^{-1} Raman band is not yet well established in the literature. In Fig. 5 this band was deconvoluted into two Gaussian curves. The insertion of a third Gaussian would result in a better fit of this band. The same band is also present in the Raman spectra of $xNa_2O \cdot (1-x)SiO_2$ glasses,[32,36–40] as well as in other glasses with ternary composition close to the disilicate and trisilicate. Its origin is related to the decrease in polymerization of the SiO_2 network due to an increase in the concentration of modifier cations. The band shifts to higher frequencies as the concentration of modifier cations is increased,[32,36–40] but its asymmetric shape changes little. The low depolarization ratio of this band in $Na_2O \cdot SiO_2$ glass[39] indicates that the vibrations giving rise to it are symmetric.

The 625 cm^{-1} Raman band has different assignments in the literature. Mysen *et al.*[32] attributed it to symmetric bending of NBO, while Furukawa *et al.*[41] consider it as stretching plus bending of Si–O–Si bands. According to the infrared band assignments (Sec. IV.B), this band is due to symmetric stretching of BO. However, the stretching motion of the Si–O bond is coupled to that of adjacent Si–O bond, where the oxygen is common to both bonds. McMillan[30] shows that the out-of-phase stretching of two adjacent Si–O bonds gives a high frequency resultant oxygen motion parallel to the Si–Si line, while the in-phase stretching of these adjacent bonds gives a low frequency resultant oxygen motion in the direction perpendicular to the Si–Si line. The in-phase stretching produces a change

in the Si–O–Si bond angle, which can be viewed as a bending motion. This agrees with the above-mentioned assignment for the infrared band and that made by Furukawa *et al.*[41] for glasses with compositions near that of the metasilicate in the Na_2O–SiO_2 glass system.

D. Microprobe Raman spectroscopy

The microprobe Raman spectra of partially and highly crystallized N_2CS_3 samples are shown in Fig. 6. They were obtained with the confocal laser Raman equipment.

Spectrum (a) was measured with the exciting laser light falling on the amorphous phase of the partially crystallized sample. It shows small differences with respect to the spectrum of the amorphous sample obtained by conventional Raman spectroscopy (Fig. 4): (i) a 25% width reduction of the 980 cm^{-1} band, (ii) a smaller relative intensity of the bands at 856 and 617 cm^{-1}, and (iii) a shift of about 8 cm^{-1} to lower frequencies of the 617 cm^{-1} band. These differences can be attributed to the scattering of surface and near-surface bond vibrations of the amorphous phase in the partially crystallized sample, while the conventional Raman spectrum is essentially due to bulk bond vibrations.

Spectrum (c) in Fig. 6, obtained for the highly crystallized sample, is typical of a polycrystalline material, as can be seen in the spectra presented by Matson *et al.*[42] for cesium and rubidium disilicates, Brawer and White[36] for alkali meta- and disilicates, and Sharma *et al.*[43] for some polymorphism of SiO_2. The two prevailing bands in this spectrum are narrower than those of spectrum (a). The band at 982 cm^{-1} is slightly shifted to higher frequencies, and the band at 592 cm^{-1} is shifted by 25 cm^{-1} to lower frequencies with respect to the amorphous phase spectrum (a). The low intensity bands at frequencies below 550 cm^{-1} have a more complex structure.[36]

As shown earlier, a distribution of SiO_4 tetrahedra with 1, 2, 3, and 4 NBO is responsible for the Raman bands observed in the frequency range between 800 and 1200 cm^{-1} of bulk N_2CS_3 glass (Fig. 4). During the glass crystallization the number of SiO_4 tetrahedra with 1, 3, and 4 NBO is reduced, and according to reactions (3) and (4) the number of tetrahedra with 2NBO should increase, until all tetrahedra have 2NBO and are rearranged in chains. As the symmetric stretching vibration of tetrahedra with 2NBO was attributed to the deconvoluted I_5 band with maximum at 975 cm^{-1} [Fig. 5(a)], it can be inferred that the band at 982 cm^{-1} of the polycrystalline N_2CS_3 sample in Fig. 6(c) is due to the same tetrahedra vibrational mode. The weak band at 910 cm^{-1} and the shoulder at 1025 cm^{-1} can be attributed to symmetric stretching vibrations of the remaining tetrahedra with 3 and 1 NBO, respectively.

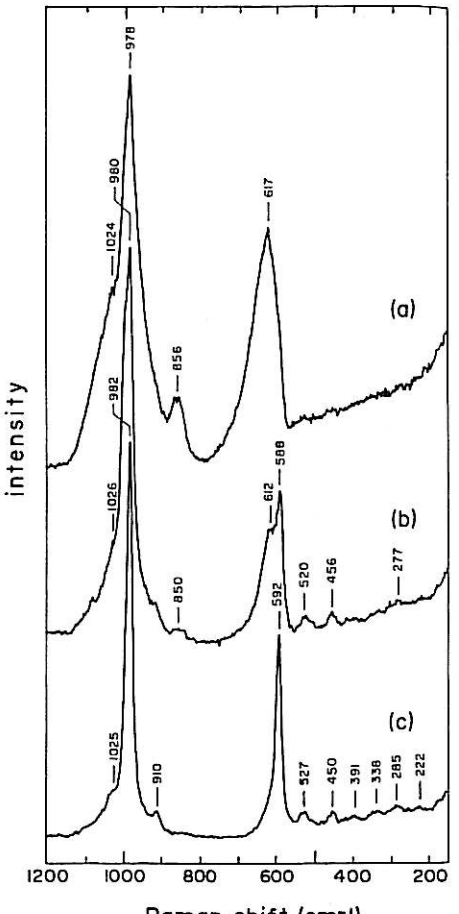

FIG. 6. Microprobe Raman spectra of (a) amorphous and (b) crystalline phases of a partially crystallized N_2CS_3 sample thermally treated at 590 °C for 15 min, and of a highly crystallized sample (c) with thermal treatment at 513 °C for 16 h.

The band at 860 cm^{-1} due to the symmetric stretching of tetrahedra with 4 NBO has completely disappeared during crystallization, as expected. The infrared activity of this tetrahedra vibration is also considerably reduced in the spectra of the polycrystalline sample, as shown in Fig. 3.

Brawer[44] presents a Raman spectrum of a polycrystalline sodium metasilicate sample, $Na_2O \cdot SiO_2$ (NS), which shape is very similar to the highly crystallized N_2CS_3 sample spectrum [Fig. 6(c)]. Apart from the differences in the band positions of both spectra, the base widths of the Raman bands of the polycrystalline NS are narrower, as expected for samples of high crystallinity, although no mention about the crystal morphology and crystallinity was made by him. Probably the polycrystalline NS sample has a crystallinity higher than that of the considered fully crystallized N_2CS_3 sample, which Raman band base widths are broader. This means that the polycrystalline N_2CS_3 sample has some residual amorphous phase. The x-ray diffraction pattern (Fig. 2) shows no indication of such residues; this technique is, however, insensitive for very small volume fractions of amorphous phase in a crystalline sample. Zanotto and James[45] studied the crystallinity, by x-ray diffraction measurements, of thermally treated $BaO \cdot 2SiO_2$ glass, where the crystals grow as spherulites. They show that the crystallinity of samples with long-time thermal treatments was not higher than 64%.

Spectrum (b) in Fig. 6 was obtained by inciding the laser light on a spherulite of the partially crystallized sample. Spectra of other spherulites are essentially the same. This spectrum shows intermediary characteristics to that of spectra (a) and (c).

Assuming that spectrum (b) is a linear combination of spectra (a) and (c), it can be written:

$$I_b = xI_a + (1 - x)I_c, \qquad 0 \leq x \leq 1 \qquad (5)$$

where I_a, I_b, and I_c are the normalized intensities of spectra (a), (b), and (c), respectively. The spectrum I_b shown in Fig. 7 is obtained for $x = 0.45$ and has practically the same shape as the measured spectrum (b) of a spherulite (Fig. 6).

From this analysis it can be asserted that the spherulites in the partially crystallized sample are not completely crystalline, having residues of an amorphous phase whose composition is probably the same as the precursor glass.

E. N_2CS_3 glass surface composition

The Raman microprobe technique gives information about the surface and near-surface bond vibrations since the focal cylinder of the incident laser light, formed by the optical microscope objective, has a typical diameter and length of about 1 μm and 2.5 μm, respectively. This small volume concentrates the maximum irradiance of the incident light and is focused at the surface of the sample.

In Sec. IV.D some differences between the Raman spectra of N_2CS_3 glass obtained in conventional 90° (Fig. 4) and in backscattering geometry with the microprobe technique [Fig. 6(a)] have been discussed. One cause of these differences was attributed to the distinct

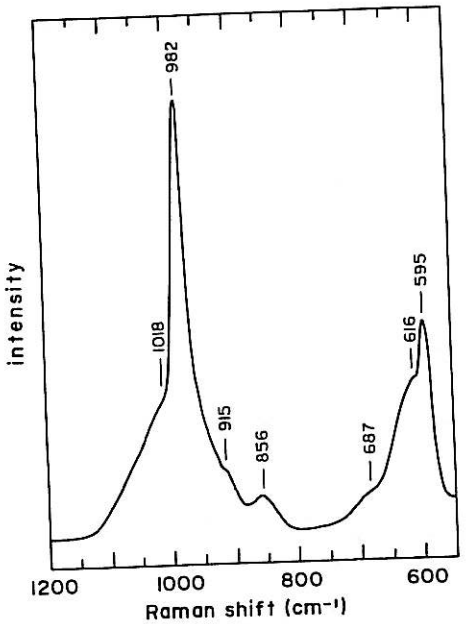

FIG. 7. Resulting spectra I_b taking $x = 0.45$ in Eq. (5), and using the intensities I_a and I_c of the spectra (a) and (c) of Fig. 6.

vibrational behavior of bulk and surface bonds, since bulk and surface structures are not the same.[25] This is due to differences in the composition in both regions.[46,47]

Pantano *et al.*[46] measured the composition profile of a commercial soda-lime-silica glass by Auger electron spectroscopy. The glass studied had 74 mol% of SiO_2, and thus with a high degree of polymerization. An ion-milled sample exposed to air for 5 min shows a higher concentration of Na_2O at the surface than in the bulk. This is due to reactions of atmospheric water vapor with the glass surface, resulting in a sodium hydroxide surface layer. The surface enrichment with sodium gives rise to a depleted region beneath the surface, which in turn hinders the diffusion of additional Na ions to the surface. As Ca ions are tightly bonded to the glass structure, their diffusion to the surface is less pronounced.

The N_2CS_3 glass is less polymerized than the glass studied by Pantano *et al.*,[46] and the surface reactions with atmospheric water are faster. This has been observed with optically polished surfaces exposed to air: after exposure of some hours or days, depending on the atmospheric relative humidity, the polished surface becomes whitish and opaque due to formation of small needle-like crystals, as observed by optical microscopy,

probably sodium hydroxide. In such a glass the depleted region is believed to be deeper than in high-silica glasses.

These considerations lead one to suppose that the Raman microprobe technique is sensitive to surface composition of glasses.

Figure 8 shows a comparison of bulk Raman spectra of some metasilicate glasses with those of bulk and surface spectra of the N_2CS_3 glass, where the differences between both of the latter spectra become meaningful.

The bands of the CS spectrum have higher intensity than the others. It seems to be exaggerated below 800 cm^{-1}, but such behavior has also been observed by Virgo *et al.*[31] and Yin *et al.*[49]

N_2CS_3 glass has an intermediate composition between that of the NS and CS glasses. As Na_2O is added to CS glass, the Raman relative intensity of the glasses decreases. The lower relative intensity is attained for the NS glass. For a glass with composition $1Na_2O \cdot 2CaO \cdot 3SiO_2$, the Raman spectrum intensity lies between those of the CS and N_2CS_3 glasses.[7] The intensity of the N_2CS_3 surface spectrum is intermediary to that of the N_2CS_3 and NS bulk spectra. This is a clear indication that the surface and near-surface of the N_2CS_3 glass have different composition from that of the bulk, and that it has a higher Na ion concentration. This result is in agreement with the results presented by Pantano *et al.*[46]

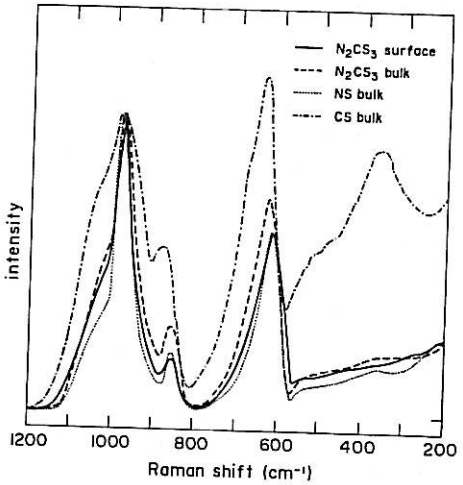

FIG. 8. Superposition of Raman spectra of some metasilicate glasses: amorphous phase of partially crystallized N_2CS_3 [from Fig. 6(a)], bulk N_2CS_3 glass (from Fig. 4), bulk $Na_2O \cdot SiO_2$ (NS) glass,[44] and bulk $CaO \cdot SiO_2$ (CS) glass.[48] The spectra are normalized with respect to the maximum of the 980 cm^{-1} band.

An increase in the sodium concentration at the glass surface can be attributed to the occurrence of a diffusional process of those ions from the bulk to the surface, as a result of superficial reactions. Dunken[25] and Doremus[50] discussed some characteristic reactions that can take place at glass surfaces, and their influence in the diffusion of specific ions through glass-solution and glass-vapor interfaces.

Since the preparation of the N_2CS_3 samples to the Raman measurements, several processes took place with some type of surface reaction, of more or less intensity: (i) leaching during grinding (lapping) and polishing; the final slurry became highly alkaline; (ii) etching for 10 s in acid solution; (iii) a long time (6 weeks) elapsed between etching and Raman measurements; (iv) weathering occurred during this time, although the samples have been conditioned in a recipient with silica-gel. A diffusional process promoted by reactions involved in some of those situations could have produced the surface and near-surface increase in the Na ions concentration.

In order to verify if such diffusion can actually happen under the situations exposed above, systematic experimental measurements are needed to determine the compositional profile of such less polymerized glasses, where it is to be expected that the variations of composition extend deeper than for high-silica glasses.

V. CONCLUSIONS

The increasing crystallinity of the N_2CS_3 glass with thermal treatments was observed by x-ray diffraction, infrared and microprobe Raman spectroscopy measurements, and scanning electron microscopy observations. The x-ray diffractograms of highly crystallized samples show no evidence of reminiscent amorphous phase which leads us to conclude that the sample is polycrystalline and has 100% crystallinity. Infrared measurements and scanning electron microscopy observations are insensitive to lead to such a conclusion, but the microprobe Raman measurements show that highly crystallized samples have, as a matter of fact, a very low concentration of a residual amorphous phase embedded in the crystal phase. This was established by the observation that the basis of the Raman bands is broader than for full crystalline materials.

The microprobe Raman spectra show clearly that the spherulites are constituted by crystalline and amorphous phases. The degree of crystallinity of these spherulites could be determined if the actual fully crystallized sample spectrum is known.

The densities of N_2CS_3 glass and of maximum crystallized samples are (2.661 ± 0.003) and (2.759 ± 0.009) g/cm^3, respectively.[7] This means that the Si–O (BO and NBO) bond lengths are shortened with increasing crystallinity. The strengthening of these bonds also increases, where the Si–NBO bonds are stronger than the Si–BO bonds.[51] These considerations probably account for the low shift of the 970 cm^{-1} Raman band and of the main high frequency infrared bands to higher frequencies as the crystallinity increases.

The structural changes which accompany the increasing crystallinity may be the reason for the shift of the 620 cm^{-1} Raman band to lower frequencies.

An interesting feature observed in the comparison of the metasilicate glasses Raman spectra is that the microprobe Raman technique seems to be able to give information about the compositional changes and bond vibrations at the materials surfaces.

ACKNOWLEDGMENTS

The authors wish to thank Dr. J.E.C. Moreira, Dr. J. Mendes Fº, and Dr. F.E.A. Melo, Universidade Federal do Ceará (Brazil), for helpful discussions about the conventional Raman measurements made there; Dr. B. Roussel and Dr. E. Silva, of DILOR (France), where the microprobe Raman spectra were measured; Dr. A.M. Plepis, IFQSC-Universidade de São Paulo (Brazil), for performing the DSC and infrared spectra measurements, and Dr. A.C.M. Rodrigues, DEMa-Universidade Federal de São Carlos, for the glass chemical analysis. This work was supported by FAPESP, FINEP, and CNPq (Brazil).

REFERENCES

1. R.L. Mozzi and B.E. Warren, J. Appl. Crystallogr. **2**, 164 (1969).
2. R. Shuker and R.W. Gammon, Phys. Rev. Lett. **25** (4), 222 (1970).
3. D.A. Long, *Raman Spectroscopy* (McGraw-Hill, London, 1977).
4. V.M. Fokin, A.M. Kalinina, and V.N. Filipovich, Sov. J. Glass Phys. Chem. **6** (2), 100 (1980).
5. A.M. Kalinina, V.N. Filipovich, and V.M. Fokin, J. Non-Cryst. Solids **38 & 39**, 723 (1980).
6. V.M. Fokin, A.M. Kalinina, and V.N. Filipovich, J. Cryst. Growth **52**, 115 (1981).
7. E.C. Ziemath, Ph.D. Thesis, Universidade de São Paulo, Brazil (1990).
8. S.W. Freiman, G.Y. Onoda, Jr., and A.G. Pincus, in *Advances in Nucleation and Crystallization in Glasses*, edited by L.L. Hench and S.W. Freiman (The American Ceramic Society, Westerville, OH, 1971), p. 141.
9. H.D. Keith and F.J. Padden, Jr., J. Appl. Phys. **34** (8), 2409 (1963).
10. W.S. McDonald and D.W.J. Cruickshank, Acta Crystallogr. **22**, 37 (1967).
11. R.M. Weston and P.S. Rogers, Mineral. Mag. **42**, 325 (1978).
12. *Powder Diffraction File*–Inorganic Volume, edited by L.G. Berry (JCPFS, Philadelphia, PA, 1983), files #10-486 and #10-489.
13. L.S. Dent Glasser and J.S. Mileson, J. Am. Ceram. Soc. **51** (1), 55 (1968).
14. C.J.R. Gonzales-Olivier, Ph.D. Thesis, Sheffield University, UK (1979).
15. R.W.G. Wyckoff and G.W. Morey, Am. J. Sci.–Fifth Series **12** (71), 419 (1926).
16. C. Kröger and J. Blömer, Z. Anorg. Allg. Chem. **280**, 51 (1955).
17. *The Aldrich Library of FT-IR Spectra*, edited by C.J. Pouchert, ed. I (Aldrich Chemical Co., Inc., Milwaukee, WI, 1985).
18. R.V. Adams, Phys. Chem. Glasses **2** (2), 39 (1961).
19. J.W. Park and H. Chen, J. Non-Cryst. Solids **40**, 515 (1980).
20. Gan Fuxi, H. Guosong, and C. Shizheng, J. Non-Cryst. Solids **52**, 203 (1982).
21. T. Uchino, T. Sakka, K. Hotta, and M. Iwasaki, J. Am. Ceram. Soc. **72** (11), 2173 (1989).
22. R.D. Husung and R.H. Doremus, J. Mater. Res. **5**, 2209 (1990).
23. J.R. Sweet and W.B. White, Phys. Chem. Glasses **10** (6), 246 (1969).
24. F. Geotti-Bianchini, L. De Riu, G. Gagliardi, M. Guglielmi, and C.G. Pantano, Glastech. Ber. **64** (8), 205 (1991).
25. H.H. Dunken, in *Treatise on Materials Science and Technology* (Academic Press, New York, 1982), Vol. 22, p. 1.
26. F. Boccuzzi, S. Coluccia, G. Ghiotti, C. Monterra, and A. Zecchina, J. Phys. Chem. **82** (11), 1298 (1978).
27. V.K. Malinovsky and A.P. Sokolov, Solid State Commun. **57**, 757 (1986).
28. V.K. Malinovsky, V.N. Novikov, P.P. Parshin, A.P. Sokolov, and M.G. Zemlyanov, Europhys. Lett. **11** (1), 43 (1990).
29. M. Hass, J. Phys. Chem. Solids **31**, 415 (1970).
30. P. McMillan, Am. Mineral. **69**, 622 (1984).
31. D. Virgo, B.O. Mysen, and I. Kushiro, Science **208**, 1371 (1980).
32. B.O. Mysen, D. Virgo, and F.A. Seifert, Rev. Geophys. Space Phys. **20** (3), 353 (1982).
33. G.J. Exarhos, in *Structure and Bonding in Non-Crystalline Solids*, edited by G.E. Walrafen and A.G. Revesz (Plenum Press, New York, 1986), p. 203.
34. B.O. Mysen, L.W. Finger, D. Virgo, and F.A. Seifert, Am. Mineral. **67**, 686 (1982).
35. J. Zarzycki, *Les Verres et l'État Vitreux* (Masson, Paris, 1982).
36. S.A. Brawer and W.B. White, J. Chem. Phys. **63** (6), 2421 (1975).
37. B.O. Mysen, D. Virgo, and C.M. Scarfe, Am. Mineral. **65**, 690 (1980).
38. M.E. Lines, J. Non-Cryst. Solids **89**, 143 (1987).
39. I.A. Mukhitdinova and O.V. Yanush, Sov. J. Glass Phys. Chem. **15** (1), 19 (1989).
40. K. Fukumi, J. Hayakawa, and T. Komiyama, J. Non-Cryst. Solids **119**, 297 (1990).
41. T. Furukawa, K.E. Fox, and W.B. White, J. Chem. Phys. **75** (7), 3226 (1981).
42. D.W. Matson, S.K. Sharma, and J.A. Philpotts, J. Non-Cryst. Solids **58**, 323 (1983).
43. S.K. Sharma, J.F. Mammone, and M.F. Nicol, Nature **292**, 140 (1981).
44. S.A. Brawer, Phys. Rev. B **11** (8), 3173 (1975).
45. E.D. Zanotto and P.F. James, J. Non-Cryst. Solids **104**, 70 (1988).
46. C.G. Pantano, Jr., D.B. Dove, and G.Y. Onoda, Jr., J. Non-Cryst. Solids **19**, 41 (1975).
47. L.L. Hench and D.E. Clark, J. Non-Cryst. Solids **28**, 83 (1978).
48. Y. Tsunawaki, N. Iwamoto, T. Hattori, and A. Mitsuishi, J. Non-Cryst. Solids **44**, 369 (1981).
49. C.D. Yin, M. Okuno, H. Morikawa, F. Marumo, and T. Yamanaka, J. Non-Cryst. Solids **80**, 167 (1986).
50. R.H. Doremus, *Glass Science* (John Wiley & Sons, New York, 1973).
51. R. Brücker, H.U. Chun, and H. Goretzki, Glastech. Ber. **51** (1), 1 (1978).